Manuscript prepared for Atmos. Chem. Phys.
with version 4.2 of the LaTeX class copernicus.cls.
Date: 25 March 2013

# Supplementary Material For: Droplet Number Uncertainties Associated With CCN: An Assessment Using Observations and a Global Adjoint Model

Richard H. Moore[1,*], Vlassis A. Karydis[2], Shannon L. Capps[1], Terry L. Lathem[2], and Athanasios Nenes[1,2]

[1]School of Chemical & Biomolecular Engineering, Georgia Institute of Technology, Atlanta, Georgia
[2]School of Earth & Atmospheric Sciences, Georgia Institute of Technology, Atlanta, Georgia
[*]Now at NASA Postdoctoral Program, NASA Langley Research Center, Hampton, Virginia

## Impact of Modeled Aerosol Concentrations ($N_a$) on Derived Cloud Droplet Concentration ($N_d$) Uncertainties

As discussed in Section 2.4 of the main article, the simulated droplet concentrations ($N_d$) typically fall within the range of observed CCN concentrations ($N_{CCN}$) for all but a few studies; although, the wide range of observed CCN concentrations indicates high levels of spatio-temporal variability in some locations that is not expected to be captured well by the GMI model analysis due to the coarse grid size and annualized data averaging. Given this variability, it is important to evaluate the robustness of derived $N_d$ uncertainties under non-climatological aerosol loadings. To assess this, additional adjoint model runs were conducted with twice and one-half the aerosol concentrations outputted by the GMI model in order to quantify how transient aerosol concentrations (0.5-times and 2-times the climatological mean) affect the derived sensitivities.

Figure S1 shows how the global distributions of $N_d$ and the sensitivity of $N_d$ to $N_a$ change under these conditions. As would be expected, overall global $N_d$ increase with increasing $N_a$; although the spatial patterns of $N_d$ are relatively unchanged. More substantial changes in $\partial \ln N_d / \partial \ln N_a$ are seen in Figure S1, particularly for the $1/2 N_a$ case relative to the base case, where much more of the southern hemisphere and continental regions have high $\partial \ln N_d / \partial \ln N_a$ values. Moving from the base case to the $2 N_a$ case appears to have a much lower impact on $\partial \ln N_d / \partial \ln N_a$ in the marine environment, while decreasing sensitivities slightly over the continents.

The overall impact of the simulated aerosol loading on the derived $N_d$ closure uncertainties is shown in Table S1, which is same computation as in Table 5 of the main article. Comparing the

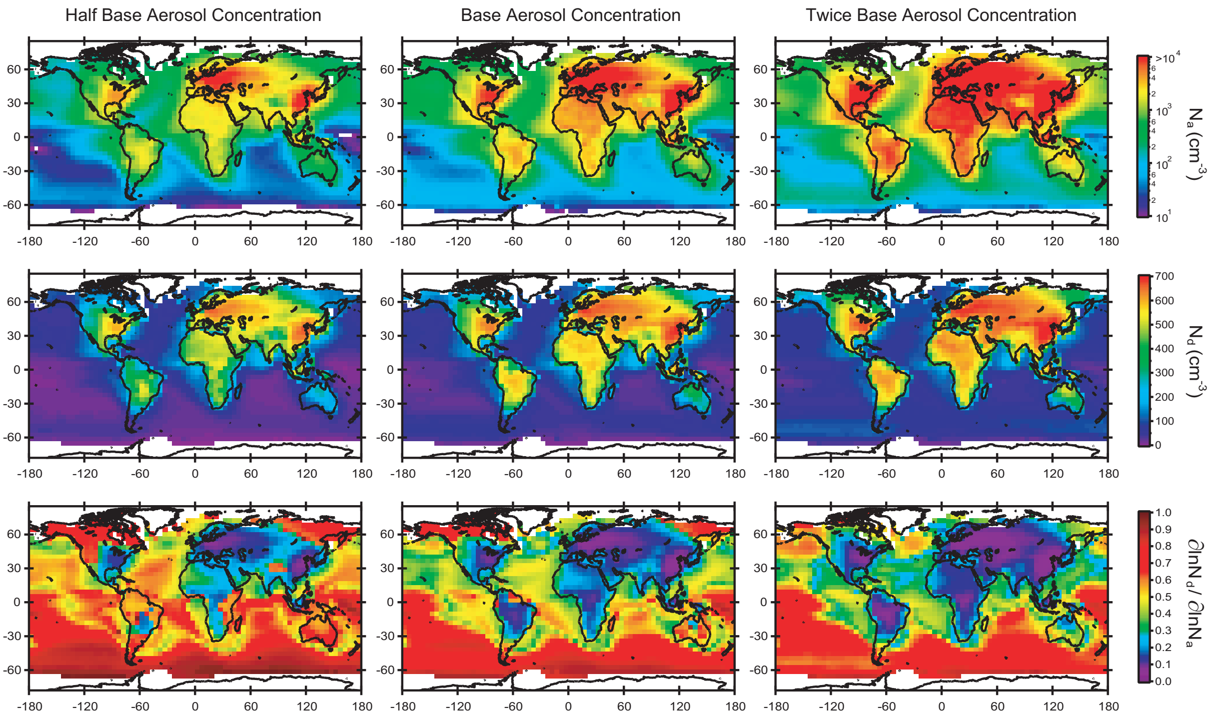


**Fig. S1.** Spatial distributions of simulated, annual-averaged $N_a$ (top), $N_d$ (middle), and sensitivity of $N_d$ to $N_a$ (bottom) for three different aerosol concentration conditions relative to the base GMI aerosol loadings.

ratio of $(\frac{\Delta N_d}{\Delta N_{CCN}})(\frac{N_{CCN}}{N_d})$ for each of the three aerosol concentration cases, it is seen that the results change significantly from the base case to the $1/2N_a$ case (from ∼0.29-0.37 to ∼0.40-0.48), while a much smaller change is observed going from the base case to the $2N_a$ case (from ∼0.29-0.37 to ∼0.25-0.32). This makes sense given that most field sites examined are within continental regions with relatively high aerosol concentrations so that a two-fold decrease in $N_a$ increases the $N_d$ sensitivity much more substantially than the sensitivity decrease associated with a two-fold increase in $N_a$ (see Figure 2 of the main article). Since spatio-temporal transients caused by local pollution sources likely increase $N_a$ relative to the base climatological condition, the results of these additional simulations indicate that the uncertainty in our analysis from the base model conditions is small (less than ∼ 5%).

**Table S1.** Variation in percent overprediction of CCN concentration$\left(\frac{\Delta N_{CCN}}{N_{CCN}}\right)$ and simulated cloud droplet concentration $\left(\frac{\Delta N_d}{N_d}\right)$ for three different aerosol concentration conditions relative to the base GMI aerosol loadings. Data are averaged over the field studies' domain, with equal weighting given to each study location regardless of area. Reported are the mean $\pm$ one standard deviation across the 36 different data sets. Since individual field studies do not apply all scenarios, the overprediction values cannot be directly compared, so domain-averaged sensitivity ratios $\left(\frac{\Delta N_d}{\Delta N_{CCN}}\right)\left(\frac{N_{CCN}}{N_d}\right)$ are also reported in parentheses.

| Closure Scenario | N | Measured Mean $N_{CCN}$ %Overprediction | Simulated Mean $N_d$ %Overprediction (Ratio) at $1/2N_{a,base}$ | Simulated Mean $N_d$ %Overprediction (Ratio) at $N_{a,base}$ | Simulated Mean $N_d$ %Overprediction (Ratio) at $2N_{a,base}$ |
|---|---|---|---|---|---|
| $(NH_4)_2SO_4$ | 16 | 59$\pm$64 | 25$\pm$35 (0.42$\pm$0.23) | 18$\pm$22 (0.31$\pm$0.16) | 15$\pm$19 (0.27$\pm$0.12) |
| Internal Mixture, Soluble Organics ($\kappa_{org}$ = 0.11) | 25 | 64$\pm$118 | 26$\pm$52 (0.42$\pm$0.21) | 21$\pm$46 (0.32$\pm$0.16) | 20$\pm$44 (0.28$\pm$0.12) |
| Internal Mixture, Insoluble Organics ($\kappa_{org}$ = 0) | 25 | 37$\pm$97 | 14$\pm$41 (0.43$\pm$0.20) | 12$\pm$36 (0.33$\pm$0.15) | 12$\pm$34 (0.29$\pm$0.12) |
| Size-Resolved, Internal Mixture, Insoluble Organics ($\kappa_{org}$ = 0) | 11 | 4$\pm$15 | 3$\pm$8 (0.40$\pm$0.20) | 1$\pm$5 (0.29$\pm$0.12) | 1$\pm$4 (0.25$\pm$0.09) |
| External Mixture, Soluble Organics ($\kappa_{org}$ = 0.11) | 17 | 71$\pm$115 | 27$\pm$49 (0.48$\pm$0.20) | 23$\pm$43 (0.37$\pm$0.15) | 22$\pm$42 (0.32$\pm$0.12) |
| External Mixture, Insoluble Organics ($\kappa_{org}$ = 0) | 16 | 16$\pm$104 | 6$\pm$49 (0.45$\pm$0.20) | 7$\pm$42 (0.33$\pm$0.14) | 7$\pm$39 (0.30$\pm$0.11) |